THE JOURNAL OF PHYSICAL CHEMISTRY B

ARTICLE

pubs.acs.org/JPCB

Spin-Selective Correlation Experiment for Measurement of Long-Range *J* Couplings and for Assignment of (*R*/*S*) Enantiomers from the Residual Dipolar Couplings and DFT

Nilamoni Nath[†,‡,§] and N. Suryaprakash[*,‡]

[†]Solid State and Structural Chemistry Unit and [‡]NMR Research Centre, Indian Institute of Science, Bangalore 560012, India

Supporting Information

ABSTRACT: We report the C-HETSERF experiment for determination of long- and short-range homo- and heteronuclear scalar couplings ($^nJ_{HH}$ and $^nJ_{XH}$, $n \geq 1$) of organic molecules with a low sensitivity dilute heteronucleus in natural abundance. The method finds significant advantage in measurement of relative signs of long-range heteronuclear total couplings in chiral organic liquid crystal. The advantage of the method is demonstrated for the measurement of residual dipolar couplings (RDCs) in enantiomers oriented in the chiral liquid crystal with a focus to unambiguously assign *R*/*S* designation in a 2D spectrum. The alignment tensor calculated from the experimental RDCs and with the computed structures of enantiomers obtained by DFT calculations provides the size of the back-calculated RDCs. Smaller root-mean-square deviations (rmsd) between experimental and calculated RDCs indicate better agreement with the input structure and its correct designation of the stereogenic center.

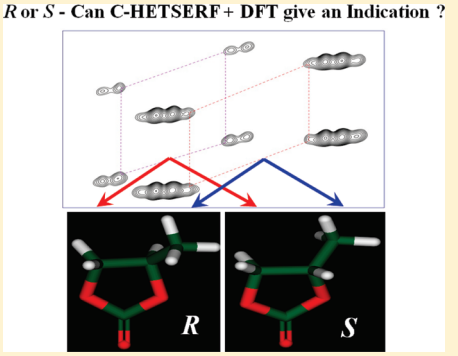

INTRODUCTION

The knowledge of short- and long-range heteronuclear coupling constants is invaluable in the study of a variety of problems in organic and inorganic chemistry.[1] The use of long-range heteronuclear couplings has received growing attention for the determination of the relative stereochemistry, structural and conformational analysis of organic and biomolecules in association with $^1H-^1H$ scalar couplings, and NOE restraints.[2,3] Furthermore, employment of the long-range heteronuclear couplings can significantly refine the computationally determined three-dimensional solution structures.[4] However, these couplings are very small in magnitude and more so are associated with low-sensitivity nuclei such as ^{13}C or ^{15}N. The routine use of such couplings is hindered by the inherent difficulties in their measurement.[5] Therefore, there is a dire need to develop simple and elegant NMR methods to measure these couplings with high accuracy. A myriad of NMR experiments viz, HSQC-TOCSY, 2D hetero-half-filtered TOCSY (HETLOC), phase-sensitive HMBC (PS-HMBC), long-range-optimized HSQC, etc., have been reported for such a purpose.[5−9] Recently, the IPAP-HSQMBC experiment for determination of long-range *J* couplings from the spin-state-selective multiplets has been demonstrated.[10] The naturally abundant ^{13}C edited selectively excited multiple quantum techniques for extraction of homo- and heteronuclear couplings have also been reported.[11]

Residual dipolar couplings (RDCs) are considered as global parameters in studying structures and conformations of proteins and conformational analysis of oligosaccharides.[13,14] The diverse aligning media with a low-order parameter for molecules soluble in polar or nonpolar medium and several weakly orienting chiral solvents for discrimination of enantiomers have been reported.[14−19] More recently, the RDCs have also been widely employed for the assignment of diastereotopic protons and for determination of the absolute configuration of organic molecules.[14,20,21] The complexity of NMR spectra of organic molecules embedded in low-ordered anisotropic solvent depends on the degree of alignment induced. In spite of the first-order splitting pattern in these media, the ^1H spectra are undecipherable even for a very small molecule containing 5−6 coupled protons.[11] Therefore, extraction of both long-range homo- and heteronuclear RDCs is a challenging task.

In the present study we demonstrate the application of a simple two-dimensional C-HETSERF experiment[22] whose pulse sequence consists of two independent and well-differentiated parts. The first part is INEPT transfer to create the ^{13}C-bound proton signal, which is subsequently subjected to evolve under all the possible homo- and heteronuclear couplings in both dimensions. In the second part, a small flip angle pulse is used before detection in order to obtain simplified E-COSY-type multiplet patterns. The selective pulse applied to select a bunch of frequencies prior to the indirect dimension has no role to simplify the spectrum. Nevertheless, simplification of the complex multiplet pattern depends only on the small angle mixing pulse.[22] Therefore, the selective $\pi/2$ pulse is replaced by a nonselective $\pi/2$ pulse to cover the entire spectral range, enabling determination of all the couplings in a single experiment. The significant advantage of the experiment is in

Received: December 31, 2010
Revised: April 26, 2011
Published: May 10, 2011

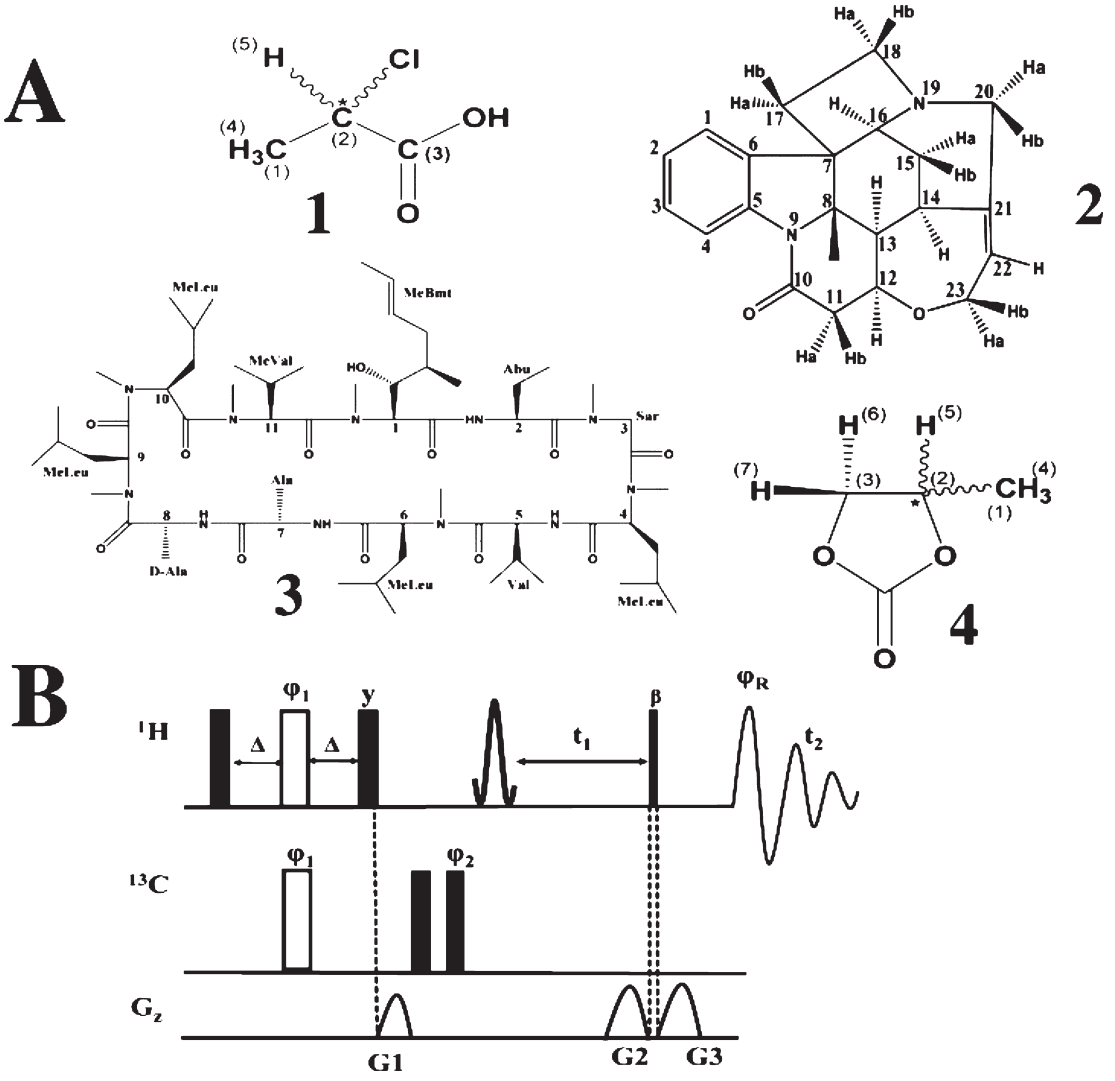

Figure 1. (A) Structures of **1**, **2**, **3**, and **4**. (B) C-HETSERF sequence.[22] Filled rectangles denote 90° pulses; open rectangles denote 180° pulses. The $\pi/2$ pulse before t_1 delay is semiselective. Unless specified, the phase of the pulses is x. The phases of the pulses are $\varphi_1 = 2(x), 2(-x)$, $\varphi_2 = \varphi_R = x, -x$. The mixing pulse applied on the proton is a small angle pulse. This small angle (β) employed for the all the experiments is 26°. The INEPT transfer delay Δ is $1/(4 \times {}^1J_{CH})$. The gradients strengths are G1 = 10 G/cm and G2 = G3 = 5 G/cm.

the relative displacement of the spin-state-selective ^{13}C α/β cross peaks facilitating extraction of long-range heteronuclear J couplings of very small magnitudes.

EXPERIMENTAL SECTION

For isotropic studies, three molecules, viz., 2-chloropropanoic acid (**1**), the alkaloid strychnine (**2**), and an undecapeptide cyclosporine A (**3**), were investigated in $CDCl_3$. The solutions of (*R/S*)-propylene carbonate (**4**) were prepared in both liquid crystalline and isotropic solvents. For the liquid crystalline phase, organic homopolypeptide, poly-γ-benzyl-L-glutamate (PBLG) and the solute were dissolved in $CDCl_3$ using a well-documented procedure.[23,24] For the *R/S* assignment of the enantiomers, a sample of **4** enriched with *R* enantiomer was prepared. For the aligned sample **4**, 54 mg of the solute mixture (32 mg of *R* and 20 mg of *S*) and 102.8 mg of PBLG and 665 mg of $CDCl_3$ were taken. For demonstrating the advantage of the experiment in determination of signs of couplings, the oriented sample of a racemic **1** was also prepared. The composition of the oriented racemic sample **1** was 50 mg of the solute, 80 mg of PBLG, and 300 mg of $CDCl_3$. The spectra were recorded either on a Bruker AV800 MHz NMR spectrometer equipped with a TCI cryogenic probe or on a Bruker DRX 500 MHz NMR spectrometer equipped with a TXI probe. The temperature was regulated by using a standard variable-temperature unit (BVT 3000). The C-HETSERF pulse sequence employed is depicted in Figure 1B. The delay "Δ" responsible for creation of the ^{13}C-bound proton signal was kept at 1.78 ms in isotropic studies. The value of "Δ" for oriented samples and other experimental and processing parameters are provided in the respective figure captions. The 2D spectra of **3** and **4** are provided in the Supporting Information along with their analysis.

RESULTS AND DISCUSSIONS

One of the difficulties associated with measurement of the long-range couplings is their very small magnitudes. Measurement of the separation between two lines (i.e., coupling) is difficult when they are in close proximity or overlapped in a single cross section of

dx.doi.org/10.1021/jp112416q |*J. Phys. Chem. B* 2011, 115, 6868–6875

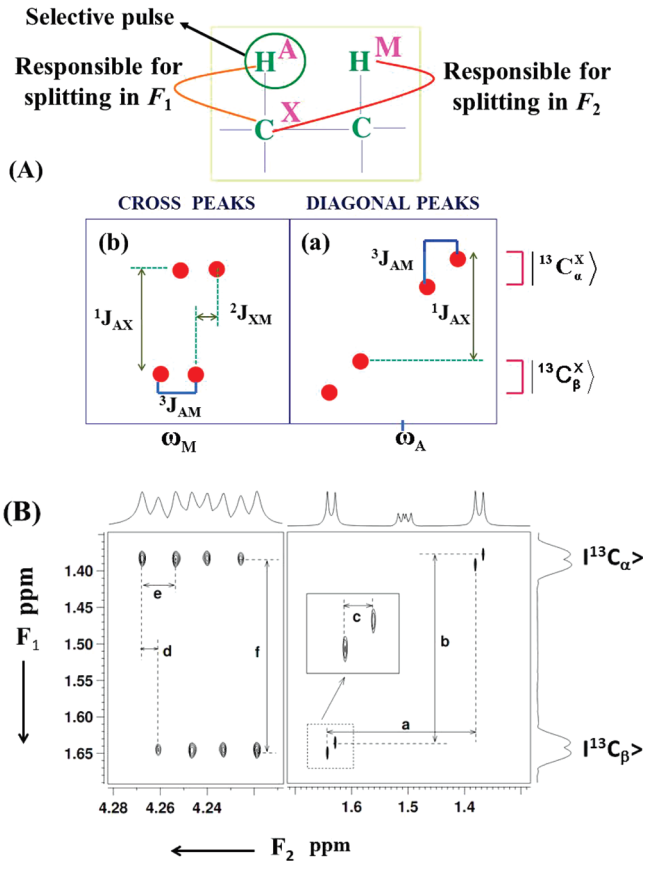

Figure 2. (A) Pictorial depiction of the extraction of different couplings from C-HETSERF experiment. (a) The diagonal peaks yielding the one-bond heteronuclear couplings. It is the frequency difference between the ^{13}C-bound proton signals at their $|^{13}C_\alpha\rangle$ or $|^{13}C_\beta\rangle$ spin states in both dimensions. (b) Cross peaks yielding the long-range heteronuclear couplings. F_2 cross section of the ^{13}C-attached proton signals at either $|^{13}C_\alpha\rangle$ or $|^{13}C_\beta\rangle$ states provide the homonuclear couplings. (B) 500 MHz 2D methyl-selective C-HETSERF spectrum of **1**. $|^{13}C_\alpha\rangle$ and $|^{13}C_\beta\rangle$ regions are marked. SEDUCE-shaped pulse of duration 3.125 ms was applied on the methyl protons. Eight scans were accumulated for each of the 128 t_1 increments, and the number of the data points in t_2 was 10 240. The spectral widths in the $F_1$and F_2 dimensions are 300 and 2000 Hz, respectively. Zero filling to 512 in F_1 and 16 384 points in F_2 and sine squared function in both dimensions were applied before processing. The recycle delay was 3 s. The magnitudes (in Hz) of J couplings are $a = b = f = {}^1J_{C1H4} = 131.2$, $c = e = {}^3J_{H4H5} = 7.3$, and $d = {}^2J_{C1H5} = 3.4$.

a 2D spectrum. However, the coupling of smaller magnitude can be determined if the peaks are made to appear in different cross sections. This unique feature, being present in the C-HETSERF experiment owing to the spin-state selection by the ^{13}C nuclei, allows determination of very small long-range heteronuclear couplings.[22] To demonstrate the outcome of the C-HETSERF experiment, an AMX spin system as shown in Figure 2A is considered where A and M are protons separated by a three-bond coupling and X is a carbon directly attached to proton A. If a selective $\pi/2$ pulse is applied on A, then spitting in the indirect dimension is due to one-bond coupling between A and X whereas the splitting in the direct dimension arises because of the long-range coupling between X and M. Extraction of three-bond coupling between A and M is derivable from both the diagonal peak and cross peaks. The appearance of the spectrum and the frequency differences yielding couplings in both diagonal and cross peaks are pictorially depicted in Figure 2A.

In order to derive better insight into the outcome of the present experiment, initially molecule **1** was investigated. The methyl-selective 2D C-HETSERF spectrum of **1** presented in Figure 2B shows diagonal peaks at the methyl proton chemical shift (δ = 1.7 ppm) and the cross peaks at the methine proton chemical shift (δ = 4.4 ppm). The ^{13}C-bound methyl proton signal evolves under $^1J_{C1H4}$ in the indirect dimension and under $^1J_{C1H4}$, $^2J_{C1H5}$, and $^3J_{H4H5}$ in the direct dimension. From the diagonal peaks, $^1J_{C1H4}$ is extractable from both dimensions and $^3J_{H4H5}$ could be measured from either of the spin states of ^{13}C. The separations marked "a" and "b" pertain to $^1J_{C1H4}$, and "c" corresponds to $^2J_{HH}$. For the diagonal peaks, larger separations in both indirect dimension and indirect dimension correspond to one-bond ^{13}C−^{1}H couplings ($^1J_{CH}$).[22] Therefore, separation "a" is equivalent to "b". From the cross peak, the long-range $^2J_{C1H5}$ is measurable from the relative displacement between the ^{13}C α/β cross peaks along the direct dimension and $^3J_{H4H5}$ can also be extracted from the splitting in one of the ^{13}C spin states. The separations yielding these values are marked as "d" and "e", respectively. Furthermore, $^1J_{C1H4}$ is also measurable from the frequency difference between the ^{13}C α/β cross peaks (marked as "f") in the indirect dimension. It is clearly evident from this discussion that analysis of the cross peaks provides all the couplings.

To demonstrate the potentiality and generality of the method, the 2D C-HETSERF experiment, performed on **2,** is reported in Figure 3. Instead of a selective pulse, a nonselective $\pi/2$ pulse was applied to excite the entire frequency range in the indirect dimension. Several representative diagonal and cross peaks marked with rectangles in the 2D spectrum have been expanded to demonstrate the applicability of the experiment in the extraction of different couplings. As an illustration, the proton magnetization bound to ^{13}C13 evolves under both the one-bond coupling of C13 with H13 ($^1J_{C13H13}$) and the two-bond coupling of C13 with H8 ($^2J_{C13H8}$) in both dimensions. The expansions "a" and "b" show the C13 to H13 and C13 to H8 correlations, respectively. The cross peaks marked with the rectangle "c" originating from the ^{13}C15-bound proton magnetization provides coupling of the diastereomeric proton H15b with its directly attached carbon C15($^1J_{C15H15b}$). Expansion of the cross peak marked with rectangle "d" exhibits a relative displacement between the ^{13}C α/β spin states pertaining to long-range coupling of the diastereomeric proton H18b with C17 ($^2J_{C17H18b}$). The expansions of the rectangles "e−h" represent the two-bond correlations, viz., H12−C11, H11b−C12, H4−C3, H3−C4, respectively, originating from the spin-state-selective displacements of the ^{13}C α/β cross peaks. The long-range correlation of H12 with C14 providing the coupling $^3J_{C14H12}$ is also marked in expansion "e". One of the important features of this experiment lies in the fact that all one-bond carbon−proton J couplings are derivable from the diagonal peaks.

The C-HETSERF experiment is very promising to measure the long-range J_{CH} of the amide proton of cyclic peptide **3.** Some of the representative diagonal and cross peaks "a−h" of the C-HETSERF spectrum of **3** are reported in Figure 4 to demonstrate the generality of the experiment in extracting various couplings. In the ^{1}H spectrum of **3**, methyl protons of Val5 show a doublet and the methyl protons directly attached to the nitrogen of the peptide bonds exhibit singlets.[25] The expanded region of a diagonal peak marked as "a" provides one-bond correlation of the methyl protons of Val5 with its directly bonded carbon. The separation between the two components of the doublet in a single cross-section of expansion "b" pertains to the three-bond coupling of the methyl protons with H$^\beta$ ($^3J_{HH}$). The peaks centered at δ = 3.8 ppm provide ^{13}C−^{1}H correlation of the

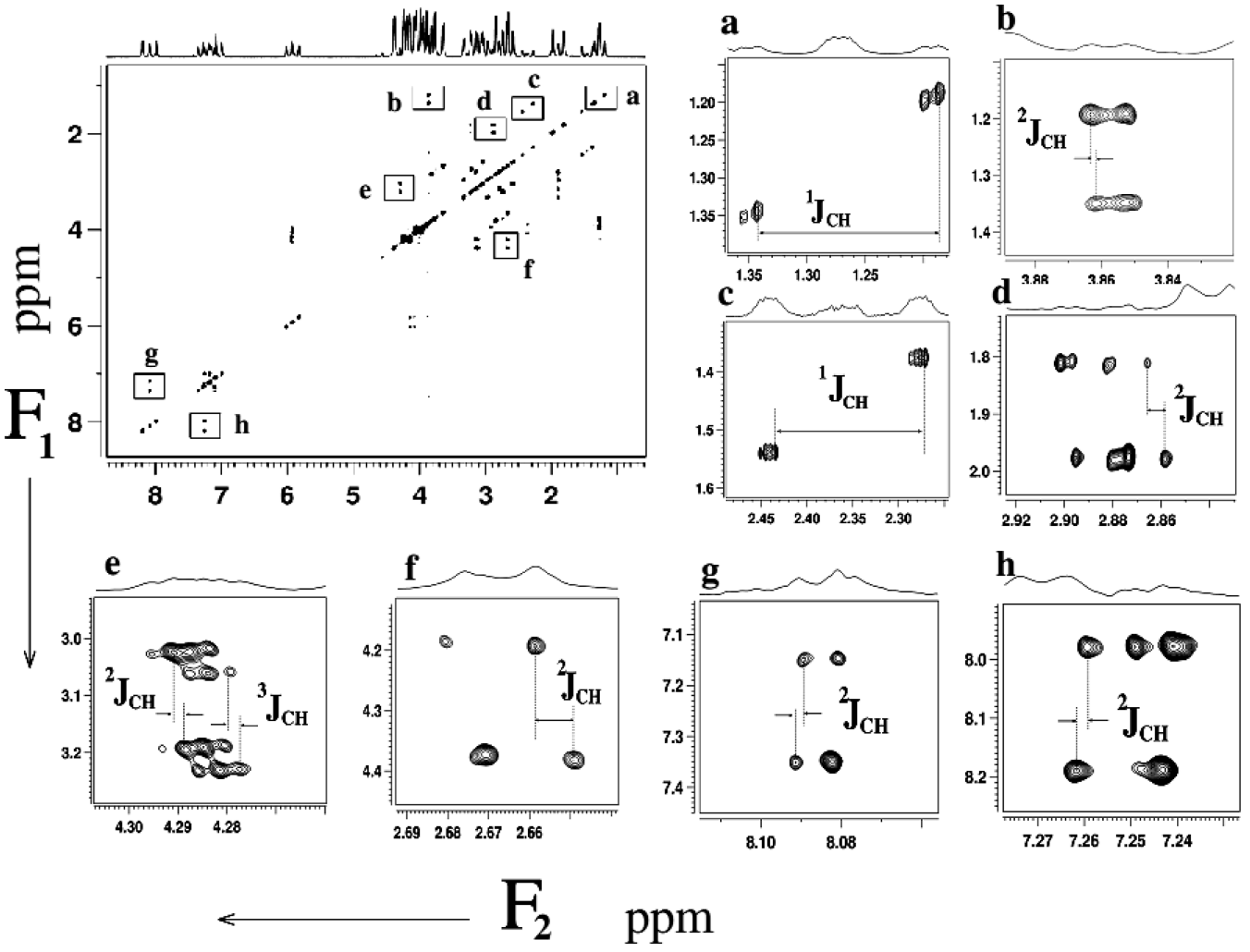

Figure 3. 800 MHz 2D C-HETSERF spectrum of **2**. Eight scans are accumulated for each of the 300 t_1 increments, and the number of data points in t_2 was 5224. The spectral widths in both dimensions were 6355 Hz. Prior to Fourier transformation, zero filling to 1024 in F_1 and 16 384 points in F_2 and sine squared window function in both dimensions were applied. The recycle delay was 3 s. The magnitudes (in Hz) of couplings are $^{1}J_{C13H13}$ = 124.1, $^{2}J_{C13H8}$ = 1.2, $^{1}J_{C15H15b}$ = 130.8, $^{1}J_{C15H15b}$ = 4.6, $^{3}J_{C14H12}$ = 1.5, $^{2}J_{C11H12}$ = 1.7, $^{2}J_{C12H11b}$ = 7.5, $^{2}J_{C3H4}$ = 1.3, and $^{2}J_{C4H3}$ = 1.9.

N-methyl group of MeBmt1($^{1}J_{CH}$). The cross peaks centered at δ = 5.8 ppm provide long-range two-bond $^{13}C-^{1}H$ coupling of C^{α} with H^{β} of the MeBmt1 (marked as "d"). The separations between spin-state-selective cross peaks "e−h" pertain to the two-bond coupling of C^{α} with the amide protons (H^{N}). These cross peaks represent the correlation of C^{α} with the amide protons of Abu2, Ala7, Val5, and D-Ala8, respectively.

Relative Signs of Long-Range Heteronuclear Couplings. For the weakly coupled spin system, the relative signs of couplings can be determined from the direction of tilt of the displacement vectors.[24] The cross peak at the methyl protons chemical shift of **1** in PBLG/$CDCl_3$ mesophase of the 2D C-HETSERF spectrum reported in Figure 5 gives additional information on the relative signs of the couplings. The displacements marked as "a" and "b" between the ^{13}C α/β cross peaks represent the three-bond long-range total coupling of methine carbon to the methyl protons for *R* and *S* enantiomers, respectively. The tilt direction at "a" is opposite to "b", indicating that coupling "a" is opposite in sign to "b".

***R/S*-Designation of the Stereogenic Center in a Chiral Molecule.** The distinction and stereochemical identification of *R*- and *S*-ibuprofen have been reported using $^{1}H-^{1}H$, $^{13}C-^{1}H$, and $^{13}C-^{13}C$ RDCs. For this purpose, the RDCs of *R*- and *S*-enantiomers have been measured for each enantiomerically pure stereoisomer aligned separately in PBLG/$CDCl_3$ mesophase.[21] To the best of our knowledge, so far the assignment of the *R* and *S* designation of enantiomers in a 2D spectrum of a racemate is arbitrary or relative. The aim of the present study is to derive the absolute configuration of enantiomers using the C-HETSERF experiment and DFT. This experiment not only discriminates the enantiomers but also enables determination of couplings.[22] For illustration, a representative region of the 2D C-HETSERF spectrum of **4** at the chemical shift position of the diastereomeric proton H6 in the PBLG/$CDCl_3$ mesophase is presented in Figure 6A. The two set of peaks pertaining to both enantiomers could be assigned in two different ways: one as in (a) a set of peaks connected by the red dashed lines could be assigned to the *R*-enantiomer while another symmetric set of peaks connected by the solid purple lines could be assigned to the *S*-enantiomer. In the other, these assignments are interchanged as in (b). With the sole objective of ascertaining the correct *R/S*-designation of the stereogenic center in a pair of enantiomers, initially the RDCs of **4** for both enantiomers and their optimized structures were determined

dx.doi.org/10.1021/jp112416q |*J. Phys. Chem. B* 2011, 115, 6868–6875

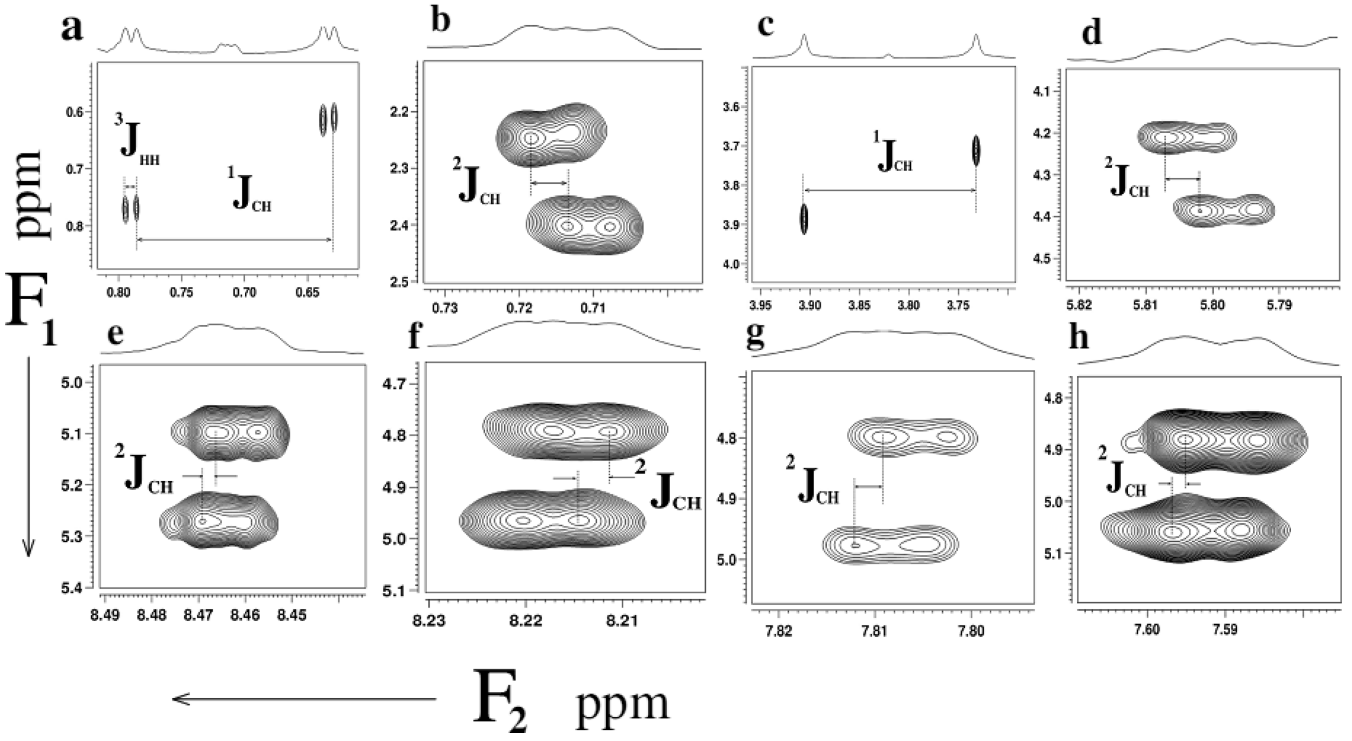

Figure 4. Diagonal peaks "a" and "c" represents one $^1J_{CH}$ and are 125.9 and 139.3 Hz, respectively. All cross peaks "b" and "d−h" represent $^2J_{CH}$, and they are 3.9, 4.3, 1.8, 2.5, and 1.3 Hz, respectively. The $^2J_{HH}$ coupling present in a single cross section of the diagonal peak marked as "a" is 6.9 Hz.

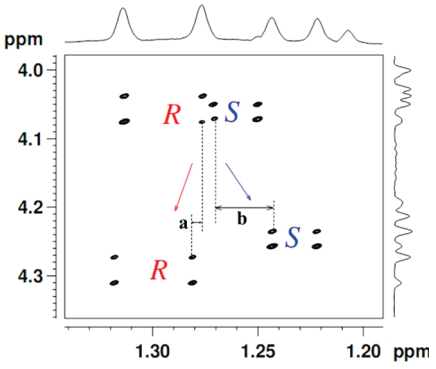

Figure 5. Cross peaks at the chemical shift of the methyl protons of the 500 MHz 2D C-HETSERF of racemate **1** in the PBLG/$CDCl_3$ solvent at 298 K. A SEDUCE-shaped pulse of 4 ms duration was applied on multiplets of the methine proton. Eight scans are accumulated for each one of the 128 t_1 increments, and the number of the data points in t_2 was set at 10 240. The spectral widths in the F_1 and F_2 dimensions are 350 and 2000 Hz, respectively. Zero filling to 512 in F_1 and 16 384 points in F_2 and sine squared function in both dimensions were applied before processing. The recycle delay was set at 3 s. The INEPT delay "$\Delta = 1/(4 \times {}^1T_{CH})$" corresponds to 1.92 ms. The magnitudes of the long-range total couplings are $a = {}^2T_{C2H4} = 2.7$ Hz for *R* and $b = {}^2T_{C2H4} = 14.0$ Hz for *S* enantiomer, respectively.

In order to determine the RDCs, two C-HETSERF experiments on **4** were performed, one in isotropic solution to determine the scalar couplings (J_{HH} and J_{CH}) and the other in anisotropic solution to obtain the total coupling constants (T_{HH} and T_{CH}). Finally, the RDCs (D_{exp}) were calculated using the simple relation $|T| = |J + 2D|$. Analysis of the C-HETSERF spectrum of **4** provides two sets of RDCs that are listed in Table 1. The regions of the spectrum facilitating extraction of these couplings are provided in the Supporting Information. One-bond $^{13}C-^{13}C$ RDCs provided in Table 1 were calculated from the INADEQUATE spectrum[26] of (*R/S*)-propylene carbonate recorded in both $CDCl_3$ and the PBLG/$CDCl_3$ mesophase. The traces from the two-dimensional $^{13}C-^{13}C$ INADEQUATE experiment showing $^1T_{CC}$ and $^1J_{CC}$ are provided in the Supporting Information. For optimization of the structures, calculations were performed using density functional theory employing B3LYP hybrid functional with a 6-311+G** contracted basis set using the program Gaussian03.[27−29] The solvent effects were examined using the polarizable continuum model (PCM) with chloroform as a solvent.

Initially, eight couplings for set I and set II were used for calculation of its alignment tensor using the PALES program[30,31] with the optimized structures of (*R*)-propylene carbonate as an input structure. This provides two sets of back-calculated RDCs (D_{calcd}) as provided in Table 1. The difference in the correlation factors between the sets of experimental and the calculated RDCs are found to be very small. However, the root-mean-square deviations (rmsd) between experimental and calculated RDCs show significantly different values. Furthermore, the smaller value of rmsd is considered to be in agreement between the input structure of a molecule with its conformation and configuration.[32] Herein, the smaller value of rmsd is considered an indicator for the correctness of the input structure and its designation of the stereogenic center. The value of rmsd between the RDCs of set I and the theoretical RDCs obtained when the optimized *R* structure is employed is low, indicating the RDCs of set I belongs to the *R*-enantiomer. On the other hand, the higher value of rmsd between the RDCs of set II and the theoretical RDCs obtained when the optimized structure of *R*-structure is employed implies that assignment of the RDCs of set II to the

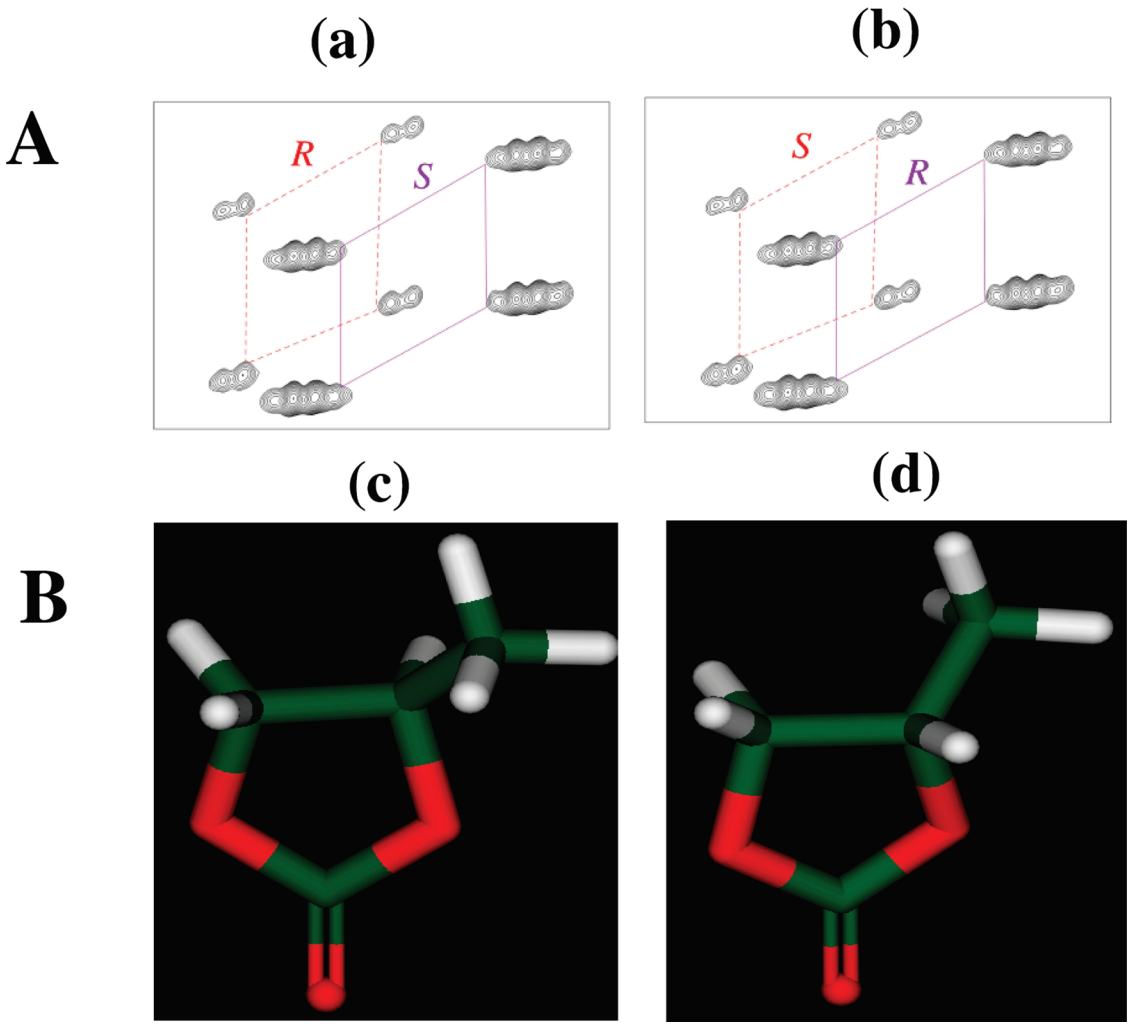

Figure 6. (A) Cross peaks of the C-HETSERF spectrum of **4** at the chemical shift position of the diastereomeric proton H6. In part a one set of symmetric peaks was assigned to the *R* enantiomer and other set of peaks to the *S* enantiomer. In part b, the assignments are interchanged. (B) (c and d) Optimized structures of (*R*)- and (*S*)-propylene carbonate, respectively, visualized in Gauss view.

Table 1. Tabulation of the Each of the Experimental and Back-Calculated RDCs Derived Using the Optimized Structure of *R* Using the PALES

	set I		set II	
coupling	experimental	[a]theoretical	experimental	[b]theoretical
C2H5	27.7	27.0	26.3	25.6
C2H7	1.9	1.2	0.00	−1.7
C2H6	2.0	−8.2	2.0	−10.8
C3H5	2.5	0.1	3.1	−2.6
C3H6	23.5	24.3	30.0	30.9
C3H7	14.5	15.1	9.4	10.3
C1C2	−9.9	−9.8	−9.2	−9.4
C2C3	−7.7	−6.8	−10.72	−9.4

[a] Theoretical RDCs when the eight RDCs of set I were used. [b] Theoretical RDCs when the eight RDCs of set II were used.

R-enantiomer is incorrect. To ascertain the consistency, in the subsequent step, the 11 couplings (provided in the Supporting Information) were employed for calculation of theoretical RDCs with the input structure of the *R*-enantiomer. This resulted in an increase in the value of rmsd since it is dependent on the number of couplings employed.[32] The smaller rmsd value between RDCs of set I and theoretical RDCs again substantiate the fact that RDCs of set I pertain to the *R*-enantiomer. It is also observed from Table 1 that the experimentally measured value of two-bond long-range coupling $^2T_{C2H6}$ is 2 Hz and the theoretical one is −8.2. This difference might arise due to the fact that the absolute sign of the two-bond carbon−proton coupling is not known. In Table 1 given in the Supporting Information, such differences arise for coupling C1H5, C1H7, and C1H6. This is probably because they are the couplings to the methyl group and there is an averaging of distances and angles for fast rotation of this methyl group.[32] Nevertheless, we used these couplings because of the limited number of couplings available for calculations, and the consistency of the larger rmsd value for the RDCs of set II is persistent. The 11 experimental and theoretical RDCs are provided in the Supporting Information. The rmsd and correlation factors for 8 and 11 couplings are provided in Table 2. The alignment tensor of the *R*-enantiomer calculated for 8 and 11 couplings separately are contained in the Supporting Information. In order to make the assignment of *R*/*S* enantiomers more

Table 2. RMSD Values and Correlation Factors between the Experimental and the Theoretically Calculated RDCs[a]

	set I with *R* structure		set II with *R* structure	
n	rmsd value	correlation factor	rmsd value	correlation factor
8	2.409	0.995	3.346	0.993
11	3.781	0.988	4.535	0.987
	set I with *S* structure		set II with *S* structure	
	rmsd value	correlation factor	rmsd value	correlation factor
8	3.326	0.993	2.381	0.995

[a] *n* is the number of couplings employed.

convincing and conclusive enough, the PALES calculations were carried out with the optimized geometry of the *S* enantiomer with both sets of experimental RDCs (set I and set II). As expected, a lower rmsd value is obtained between the experimental RDCs of set II and the theoretical RDCs, indicating that RDCs of set II belong to the *S*-enantiomer. Tables of both experimental and theoretical RDCs for the *S*-enantiomer are contained in the Supporting Information. In addition, when eight couplings with the optimized structure of the *R* enantiomer are used in PALES calculations, the difference in rmsd values is 0.937 (3.346−2.409). Almost the same difference, 0.948 (i.e., 3.329−2.381), is also obtained in rmsd values when eight couplings with the optimized structure of the *S*-enantiomer are used in PALES calculations. The optimized structures employed in the calculations for *R*- and *S*-propylene carbonate visualized in Gauss view are reported in Figure 6 B. Further confirmation of the assignment by this method was established by the methyl-selective SERF experiment (SERF spectrum and details are given in the Supporting Information).

CONCLUSIONS

The experiment employed the ^{13}C-bound proton signal for determination of short- and long-range homo- and heteronuclear *J* couplings of organic molecules with ^{13}C in natural abundance. The method finds significant advantage in determination of the relative signs of the heteronuclear long-range RDCs for enantiomers. The RDCs measured for (*R*/*S*)-propylene carbonate from a 2D spectrum and structure obtained by DFT calculations are used for calculation of the alignment tensor, which subsequently provided the possible alternate procedure for stereochemical identification of *R*- and *S*-enantiomers.

ASSOCIATED CONTENT

Supporting Information. C-HETSERF spectrum of cyclosporin-A, (*R*/*S*)-propylene carbonate, INADEQUATE spectrum of (*R*/*S*)-propylene carbonate, alignment tensor elements, table of RDCs, and SERF spectrum of (*R*/*S*)-propylene carbonate. This material is available free of charge via the Internet at http://pubs.acs.org.

AUTHOR INFORMATION

Corresponding Author

*Phone: 0091 80 22933300. Fax: 0091 80 23601550. E-mail: nsp@sif.iisc.ernet.in.

Author Contributions

§ The author carried out the experiments during his visit to Centre for Biomedical Magnetic Resonance, Sanjay Gandhi Post Graduate Institute of Medical Science Campus, Raebareli Road, Lucknow 226014.

ACKNOWLEDGMENT

Use of the NMR facility at CBMR, Lucknow, is acknowledged. The authors gratefully acknowledge Prof. C. L. Khetrapal, Director, CBMR, Lucknow, for many helpful suggestions. Vinay Ganapathy is greatly acknowledged for his help in running the PALES program, who thanks Prof. Christina M. Thiele for her help in teaching the use of the PALES program. N.N. thanks the University Grant Commission, India for a senior research fellowship. N.S. gratefully acknowledges the financial support by the Board of Research in Nuclear Sciences, Mumbai, for grant no. 2009/37/38/BRNS/2269.

REFERENCES

(1) Eberstadt, M.; Gemmecker, G.; Mierke, D. F.; Kessler, H. *Angew. Chem., Int. Ed. Engl.* **1995**, *34*, 1671–1695.
(2) Matsumori, N.; Kaneno, D.; Murata, M.; Nakamura, H.; Tachibana, K. *J. Org. Chem.* **1999**, *64*, 866–876.
(3) Bifulco, G.; Dambruoso, P.; Paloma, L. G.; Riccio, R. *Chem. Rev.* **2007**, *107*, 3744–3779.
(4) Eberstadt, M.; Mierke, D. F.; Kock, M.; Kessler, H. *Helv. Chim. Acta* **1992**, *75*, 2583–2592.
(5) Marquez, B. L.; Gerwick, W. H.; Williamson, R. T. *Magn. Reson. Chem.* **2001**, *39*, 499–530.
(6) Kover, K. E.; Hruby, V. J.; Uhrin, D. *J. Magn. Reson.* **1997**, *129*, 125–129.
(7) Uhrın, D.; Batta, G.; Hruby, V. J.; Barlow, P. N.; Kover, K. E. *J. Magn. Reson.* **1998**, *130*, 155–161.
(8) Kurz, M.; Schmieder, P.; Kessler, H. *Angew. Chem., Int. Ed. Engl.* **1991**, *30*, 1329–1331.
(9) Kozminski, W.; Nanz, D. *J. Magn. Reson.* **1997**, *124*, 383–392.
(10) Gil, S.; Espinosa, J. F.; Parella, T. *J. Magn. Reson.* **2010**, *207*, 312–321.
(11) Baishya, B.; Uday, R. P.; Suryaprakash, N. *J. Magn. Reson.* **2008**, *192*, 92–100.
(12) Kobzar, K.; Kessler, H.; Luy, B. *Angew. Chem., Int. Ed.* **2005**, *44*, 3145–3147.
(13) Tjandra, N.; Bax, A. *Science* **1997**, *278*, 1111–1113.
(14) Thiele, C. M. *Eur. J. Org. Chem.* **2008**, 5673–5685.
(15) Aroulanda, C.; Sarfati, M.; Courtieu, J.; Lesot, P. *Enantiomer* **2001**, *6*, 281–287.
(16) Vivekanandan, S.; Joy, A.; Suryaprakash, N. *J. Mol. Struct.* **2004**, *694*, 241–247.
(17) Eliav, U.; Navon, G. *J. Am. Chem. Soc.* **2006**, *128*, 15956–15957.
(18) Péchiné, J. M.; Meddour, A.; Courtieu, J. *Chem. Commun.* **2002**, 1734–1735.
(19) Sau, S.; Ramanathan, K. V. *J. Phys. Chem. B.* **2009**, *113*, 1530–1532.
(20) Thiele, C. M. *J. Org. Chem.* **2004**, *69*, 7403–7413.
(21) Marathias, V. M.; Tawa, G. J.; Golger, I.; Bach, A. C., II *Chirality* **2007**, *19*, 741–750.
(22) Nath, N.; Suryaprakash, N. *Chem. Phys. Lett.* **2010**, *496*, 175–182.
(23) Sarfati, M.; Lesot, P.; Merlet, D.; Courtieu, J. *Chem. Commun.* **2000**, 2069–2081.
(24) Prabhu, U. R.; Suryaprakash, N. *J. Magn. Reson.* **2008**, *195*, 145–152.
(25) Kessler, H.; Loosli, H. R.; Oschkinat, H. *Helv. Chim. Acta* **1985**, *68*, 661–681.

(26) Bax, A.; Freeman, R.; Kempsell, S. P. *J. Am. Chem. Soc.* **1980**, *102*, 4849.
(27) Becke, A. D. *J. Chem. Phys.* **1993**, *98*, 5648–5652.
(28) Lee, C. T.; Yang, W. T.; Parr, R. G. *Phys. Rev. B* **1988**, *37*, 785–789.
(29) Frisch, M. J.; Trucks, G. W.; Schlegel, H. B.; Scuseria, G. E.; Robb, M. A.; Cheeseman, J. R.; Montgomery, J. A., Jr.;Vreven, T.; Kudin, K. N.; Burant, J. C.; Millam, J. M.; Iyengar,S. S.; Tomasi, J.; Barone, V.; Mennucci, B.; Cossi, M.;Scalmani, G.; Rega, N.; Petersson, G. A.; Nakatsuji, H.;Hada, M.; Ehara, M.; Toyota, K.; Fukuda, R.; Hasegawa, J.;Ishida, M.; Nakajima, T.; Honda, Y.; Kitao, O.; Nakai, H.;Klene, M.; Li, X.; Knox, J. E.; Hratchian, H. P.; Cross, J. B.; Bakken, V.; Adamo, C.; Jaramillo, J.; Gomperts, R.;Stratmann, R. E.; Yazyev, O.; Austin, A. J.; Cammi, R.;Pomelli, C.; Ochterski, J. W.; Ayala, P. Y.; Morokuma, K.;Voth, G. A.; Salvador, P.; Dannenberg, J. J.; Zakrzewski, V. G.; Dapprich, S.; Daniels, A. D.; Strain, M. C.; Farkas, O.;Malick, D. K.; Rabuck, A. D.; Raghavachari, K.; Foresman,J. B.; Ortiz, J. V.; Cui, Q.; Baboul, A. G.; Clifford, S.;Cioslowski, J.; Stefanov, B. B.; Liu, G.; Liashenko, A.;Piskorz, P.; Komaromi, I.; Martin, R. L.; Fox, D. J.; Keith, T.;Al-Laham, M. A.; Peng, C. Y.; Nanayakkara, A.; Challacombe,M.; Gill, P. M. W.; Johnson, B.; Chen, W.; Wong, M. W.;Gonzalez, C.; Pople, J. A. *Gaussian 03*, Revisions B.02 and C.02; Gaussian Inc.: Wallingford, CT, 2004.
(30) Zweckstetter, M.; Bax, A. *J. Am. Chem. Soc.* **2000**, *122* 3791–3792.
(31) Zweckstetter, M. *Nat. Protoc.* **2008**, *3*, 679–690.
(32) Thiele, C M.; Marx, A.; Berger, R.; Fischer, J.; Biel, M.; Giannis, A. *Angew. Chem., Int. Ed.* **2006**, *45*, 4455–4460.